Numerical Modeling of Material Discontinuity Using Mixed MLPG Collocation Method

B. Jalušić[1], J. Sorić[1] and T. Jarak[1]

Abstract A mixed MLPG collocation method is applied for the modeling of material discontinuity in heterogeneous materials composing of homogeneous domains. Two homogeneous isotropic materials with different linear elastic properties are considered. The solution for the entire domain is obtained by enforcing the corresponding continuity conditions along the interface of homogeneous materials. For the approximation of the unknown field variables MLS functions with interpolatory conditions are applied. The accuracy and numerical efficiency of the mixed approach is compared with a standard primal meshless approach and demonstrated by a representative numerical example.

Keywords: Mixed meshless approach, MLS approximation, heterogeneous materials

1 Introduction

In recent decades, a new group of numerical approaches known as meshless methods has attracted tremendous interest due to its potential to overcome certain shortcomings of mesh-based methods such as element distortion problems and time-demanding mesh generation process. Nevertheless, the calculation of meshless approximation functions due to its high computational cost is still a major drawback. This deficiency can be alleviated to a certain extent by using the mixed Meshless Local Petrov-Galerkin (MLPG) Method paradigm [Atluri, Liu, Han (2006)].

In the present contribution, the MLPG formulation based on the mixed approach is adapted for the modeling of deformation responses of heterogeneous materials. A heterogeneous structure consists of two homogeneous materials which are discretized by grid points in which equilibrium equations are imposed. The linear elastic boundary value problem for each homogeneous material is discretized by using the independent approximations of displacement and stress components. Independent variables are approximated using meshless functions in such a way that each material is treated as a separate problem [Chen, Wang, Hu, Chi (2009)]. The global solution for the entire heterogeneous structure is acquired by enforcing appropriate displacement and traction conditions along the interface of two homogeneous materials. A collocation meshless method is used, which may be considered as a special case of the MLPG approach, where the Dirac delta function is utilized as the test function. Since the collocation method is

[1] Faculty of Mechanical Engineering and Naval Architecture, University of Zagreb, Ivana Lučića 5, 10000 Zagreb, Croatia.

employed, the strong form of equilibrium equations is yielded and time-consuming numerical integration process is avoided. The moving least squares (MLS) approximation functions [Atluri (2004)] with interpolatory properties are applied. This enables simple imposition of displacement boundary conditions as in FEM. Traction boundary conditions on outer edges are enforced via the direct collocation approach. In order to derive the final closed system of discretized governing equations with the displacements as unknown variables, the nodal stress values are expressed in terms of the displacement components using the kinematic and constitutive relations. The mixed MLPG collocation method for modeling of material discontinuity is presented and explained at large in chapter 2. Efficiency of the proposed mixed method is analyzed in detail on a well-known numerical example of a plate with circular inclusion with different material properties. In chapter 3 the accuracy of the utilized approach is also compared to a standard meshless primal approach.

2 Mixed MLPG collocation method for heterogeneous materials

The two-dimensional heterogeneous material which occupies the global computational domain Ω surrounded by the global outer boundary Γ is considered, as shown in Figure 1. The boundary Γ_s represents the interface between two subdomains Ω^+ i Ω^- with different homogeneous material properties. Γ_s separates the global domain Ω in such a manner that $\Omega = \Omega^+ \cup \Omega^-$ and $\Gamma = \Gamma^+ \cup \Gamma^-$.

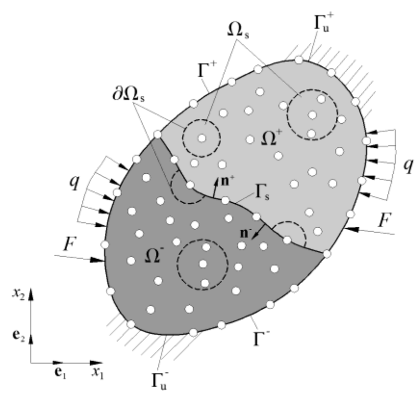

Figure 1: Two-dimensional heterogeneous material

The governing equations for the presented example are the strong form 2D equilibrium equations which have to be satisfied within the global computational domain Ω divided into Ω^+ and Ω^-

$$\sigma^+_{ij,x_j} + b^+_i = 0, \text{ within } \Omega^+, \quad \sigma^-_{ij,x_j} + b^-_i = 0, \text{ within } \Omega^-. \tag{1}$$

Equations (1) have to satisfy the boundary conditions prescribed on the local subdomain boundaries $\partial\Omega$

$$u^+_i = \bar{u}^+_i, \text{ on } \Gamma^+_u, \quad u^-_i = \bar{u}^-_i, \text{ on } \Gamma^-_u, \tag{2}$$

$$t_i^+ = \sigma_{ij}^+ n_j^+ = \bar{t}_i^{\,+}, \ \text{ on } \Gamma_t^+, \quad t_i^- = \sigma_{ij}^- n_j^- = \bar{t}_i^{\,-}, \ \text{ on } \Gamma_t^- \tag{3}$$

and interface conditions on the boundary Γ_s. For the discretization of Γ_s, the double node concept in employed. At each node on Γ_s, the interface conditions of displacement continuity and traction equilibrium are enforced

$$u_i^+ - u_i^- = 0, \quad t_i^+ + t_i^- = 0. \tag{4}$$

The external boundary of the local subdomain $\partial\Omega$ is composed of several parts, $\partial\Omega = \Gamma_u^+ \cup \Gamma_u^- \cup \Gamma_t^+ \cup \Gamma_t^-$, where $\Gamma_u = \Gamma_u^+ \cup \Gamma_u^-$ denotes the part of $\partial\Omega$ with prescribed displacement boundary conditions $\bar{u}_i$, while $\Gamma_t = \Gamma_t^+ \cup \Gamma_t^-$ denotes the part, where the traction boundary conditions $\bar{t}_i$ are applied. The two-dimensional heterogeneous continuum is discretized by two different set of nodes $I = 1,2,...,N$ and $M = 1,2,...,P$, where N and P indicate the total number of nodes within Ω^+ and Ω^-, respectively. According to the mixed collocation procedure [Atluri, Liu, Han (2006)], the unknown field variables are the displacement and stress components. All unknown field variables are approximated separately within subdomains Ω^+ and Ω^-, where the same approximation functions are employed for all the displacement and stress components. For the subdomain Ω^+ it can be written

$$u_i^{+(h)}(\mathbf{x}) = \sum_{J=1}^{N_{\Omega_s}} \phi_J(\mathbf{x}) \left(\hat{u}_i^+\right)_J, \tag{5}$$

$$\sigma_{ij}^{+(h)}(\mathbf{x}) = \sum_{J=1}^{N_{\Omega_s}} \phi_J(\mathbf{x}) \left(\hat{\sigma}_{ij}^+\right)_J, \tag{6}$$

where ϕ_J represents the nodal value of two-dimensional shape function for node J, N_{Ω_s} stands for the number of nodes within the approximation domain Ω_s, while $\left(\hat{u}_i^+\right)_J$ and $\left(\hat{\sigma}_{ij}^+\right)_J$ denote the nodal values of displacement and stress components. The displacement and stress components are analogously approximated over the subdomain Ω^-. For the shape function construction the well-known MLS approximation scheme [Atluri (2004)] is employed. The interpolatory properties of the MLS approximation function are achieved by utilizing the weight function according to [Most, Bucher (2008)]. Applying the mixed MLPG strategy the equilibrium equations (1) are discretized by the stress approximation (6), leading to

$$\sum_{J=1}^{N_{\Omega_s}} \mathbf{B}_{IJ}^{+\mathrm{T}} \hat{\boldsymbol{\sigma}}_J^+ + \mathbf{b}_I^+ = \mathbf{0}, \ \text{ within } \Omega^+, \qquad \sum_{J=1}^{N_{\Omega_s}} \mathbf{B}_{MJ}^{-\mathrm{T}} \hat{\boldsymbol{\sigma}}_J^- + \mathbf{b}_M^- = \mathbf{0}, \ \text{ within } \Omega^-, \tag{7}$$

where $\mathbf{B}_{IJ} = \mathbf{B}_J(\mathbf{x}_I)$ and $\mathbf{B}_{MJ} = \mathbf{B}_J(\mathbf{x}_M)$ indicate the matrices consisting of the first-order derivatives of shape functions. It can be verified that the number of equations at the global level obtained by (7) is less than the total number of stress unknowns. Therefore, in order to obtain the closed system of equations, the compatibility between the approximated stresses and displacements is utilized at collocation nodes

$$\hat{\boldsymbol{\sigma}}_J^+ = \mathbf{D}^+ \sum_{K=1}^{N_{\Omega_s}} \mathbf{B}_{JK}^+ \hat{\mathbf{u}}_K, \qquad \hat{\boldsymbol{\sigma}}_J^- = \mathbf{D}^- \sum_{K=1}^{N_{\Omega_s}} \mathbf{B}_{JK}^- \hat{\mathbf{u}}_K, \tag{8}$$

where $\mathbf{D}^+$ and $\mathbf{D}^-$ denote material tensors for each homogeneous domain. Inserting the discretized constitutive relations (8) into the discretized equilibrium equations (7), a solvable system of linear algebraic equations with only the nodal displacements as unknowns is attained

$$\sum_{J=1}^{N_{\Omega_s}} \mathbf{K}_{IJ}^+ \hat{\mathbf{u}}_J^+ = \mathbf{R}_I^+, \ \text{ within } \Omega^+, \qquad \sum_{J=1}^{N_{\Omega_s}} \mathbf{K}_{MJ}^- \hat{\mathbf{u}}_J^- = \mathbf{R}_M^-, \ \text{ within } \Omega^-. \tag{9}$$

In equations (9), the nodal stiffness matrices $\mathbf{K}_{IJ}^+$ and $\mathbf{K}_{MJ}^-$ are defined as

$$\mathbf{K}_{IJ}^+ = \sum_{K=1}^{N_{\Omega_s}} \mathbf{B}_{KI}^{+\mathrm{T}} \mathbf{D}^+ \mathbf{B}_{JK}^+, \qquad \mathbf{K}_{MJ}^- = \sum_{K=1}^{N_{\Omega_s}} \mathbf{B}_{KM}^{-\mathrm{T}} \mathbf{D}^- \mathbf{B}_{JK}^-, \tag{10}$$

while the nodal force vectors $\mathbf{R}_I^+$ and $\mathbf{R}_M^-$ are simply equal to

$$\mathbf{R}_I^+ = -\mathbf{b}_I^+, \qquad \mathbf{R}_M^- = -\mathbf{b}_M^-. \tag{11}$$

All approximation functions in this contribution possess the interpolation property at the nodes. Consequently, the displacement boundary conditions are enforced straightforward, analogously to the procedure in FEM. Therefore, by discretizing the displacement boundary conditions (2) with the approximation (5) we obtain

$$\bar{\mathbf{u}}_I^+ = \sum_{J=1}^{N_{\Omega_s}} \phi_J \hat{\mathbf{u}}_J^+, \quad \text{on } \Gamma_\mathrm{u}^+, \qquad \bar{\mathbf{u}}_M^- = \sum_{J=1}^{N_{\Omega_s}} \phi_J \hat{\mathbf{u}}_J^-, \quad \text{on } \Gamma_\mathrm{u}^-. \tag{12}$$

Applying the stress approximation (6) and the compatibility between the approximated stresses and displacements (8) in the boundary equations (3), the discretized traction boundary conditions are derived as

$$\bar{\mathbf{t}}_I^+ = \mathbf{N}_I^+ \mathbf{D}^+ \sum_{K=1}^{N_{\Omega_s}} \mathbf{B}_{IK}^+ \mathbf{u}_K^+, \quad \text{on } \Gamma_\mathrm{t}^+, \qquad \bar{\mathbf{t}}_M^- = \mathbf{N}_M^- \mathbf{D}^- \sum_{K=1}^{N_{\Omega_s}} \mathbf{B}_{MK}^- \mathbf{u}_K^-, \quad \text{on } \Gamma_\mathrm{t}^-. \tag{13}$$

In a similar way the applied interface boundary conditions (4) can be discretized as

$$\sum_{J=1}^{N_{\Omega_s}} \phi_J \hat{\mathbf{u}}_J^+ = \sum_{J=1}^{N_{\Omega_s}} \phi_J \hat{\mathbf{u}}_J^-, \quad \text{on } \Gamma_\mathrm{s}, \tag{14}$$

$$\mathbf{N}_I^+ \mathbf{D}^+ \sum_{K=1}^{N_{\Omega_s}} \mathbf{B}_{IK}^+ \mathbf{u}_K^+ = -\mathbf{N}_M^- \mathbf{D}^- \sum_{K=1}^{N_{\Omega_s}} \mathbf{B}_{MK}^- \mathbf{u}_K^-, \quad \text{on } \Gamma_\mathrm{s}. \tag{15}$$

3 Numerical Example

3.1 Plate with circular inclusion

A rectangular plate of 10×10 in size with the radius of embedded circular inclusion equal to 1 subjected to unit horizontal traction is considered. Owing to the symmetry, only one quarter of the plate is modeled. The discretization of a quarter of the plate Ω^- with circular inclusion Ω^+, geometry and enforced boundary condition are shown in Figure 3. This example is used as a benchmark for testing the computational strategy presented. The material properties of the plate are $E^+ = 1000$, $\nu^+ = 0.25$, while the material properties of the inclusion are $E^- = 10000$, $\nu^- = 0.3$.

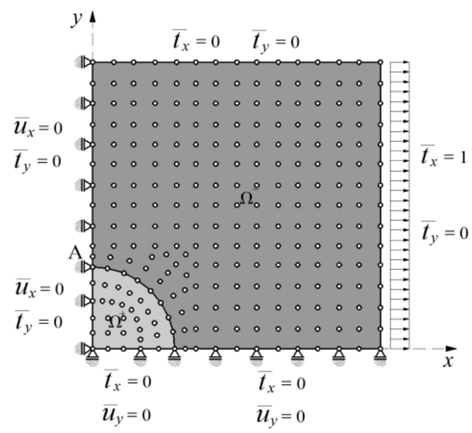

Figure 2: Plate with circular inclusion with boundary conditions

The meshless interpolation schemes using the second- and fourth-order basis (IMLS2, IMLS4) are applied and compared. Both primal (P) and mixed (M) approaches are utilized. Figures 3 and 4 show the comparison of u_y displacement and σ_x stress component distributions along $x = 0$ for model discretized with 346 nodes.

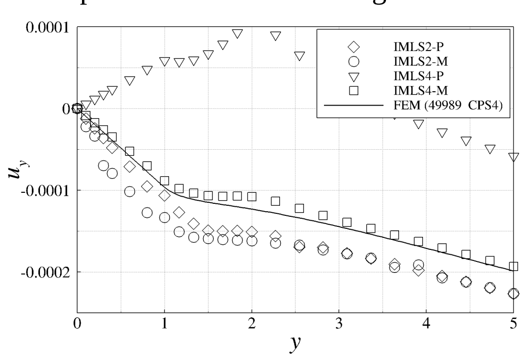

Figure 3: Displacement u_y at $x = 0$

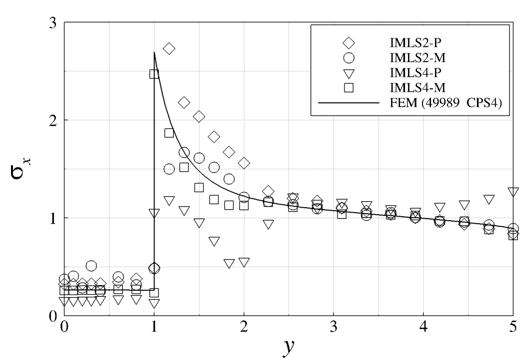

Figure 4: Stress σ_x at $x = 0$

The distributions attained are compared to referent solutions obtained by 49989 CPS4 finite elements from the finite element software Abaqus. The convergence study of both primal and mixed approaches employing the error of normalized displacement u_y and normalized stress σ_x components at point A are shown in Figures 5 and 6.

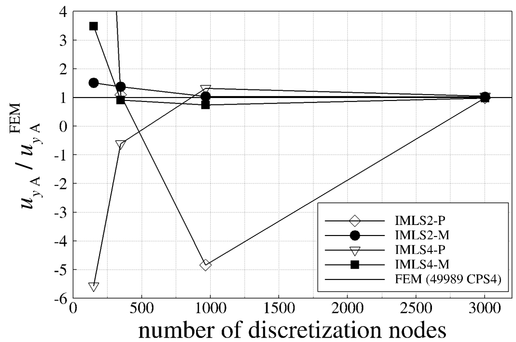

Figure 5: Convergence of normalized displacement u_y at point A

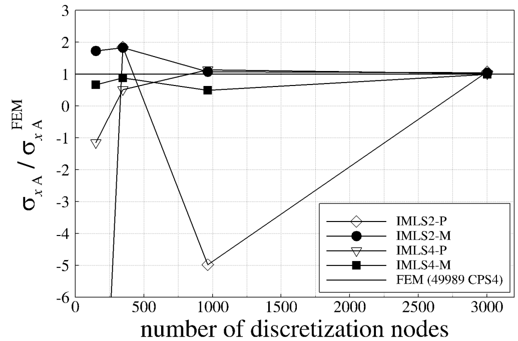

Figure 6: Convergence of normalized stress σ_x at point A

4 Conclusion

From the numerical results it can be perceived that the mixed approach is more robust and superior to the primal formulation. Therefore, a more accurate and numerically efficient modeling of heterogeneous material is achieved if the mixed meshless collocation formulation is used since it reduces the needed continuity order of the meshless approximation function to only C^1 continuity for the presented problem.

Acknowledgement This work has been fully supported by Croatian Science Foundation under the project Multiscale Numerical Modeling of Material Deformation Responses from Macro- to Nanolevel (2516).

References:

Atluri, S. N.; Liu, H. T.; Han, Z. D. (2006): Meshless Local Petrov-Galerkin (MLPG) Mixed Collocation Method for Elasticity Problems. *CMES: Computer Modeling in Engineering & Sciences*, vol. 14, no. 3, pp. 141–152.

Chen, J.-S.; Wang, L.; Hu, H.-Y.; Chi, S.-W. (2009): Subdomain radial basis collocation method for heterogeneous media. *International Journal for Numerical Methods in Engineering*, vol. 80, pp. 163–190.

Atluri, S. N. (2004): *The Meshless Local Petrov-Galerkin (MLPG) Method*. Tech. Science Press.

Most, T.; Bucher, C. (2008): New Concepts for Moving Least Squares: An Interpolating Nonsingular Weighting Function and Weighted Nodal Least Squares. *Engineering Analysis with Boundary Elements*, vol. 32, no. 6, pp. 461–470.